ACS OMEGA

http://pubs.acs.org/journal/acsodf

Article

New Natural Eugenol Derivatives as Antiproliferative Agents: Synthesis, Biological Evaluation, and Computational Studies

Syed Nazreen, Serag Eldin I. Elbehairi, Azizah M. Malebari, Nuha Alghamdi, Reem F. Alshehri, Ali A. Shati, Nada M. Ali, Mohammad Y. Alfaifi, Ahmed A. Elhenawy,* and Mohammad Mahboob Alam*

Cite This: *ACS Omega* 2023, 8, 18811−18822

Read Online

ACCESS | Metrics & More | Article Recommendations | Supporting Information

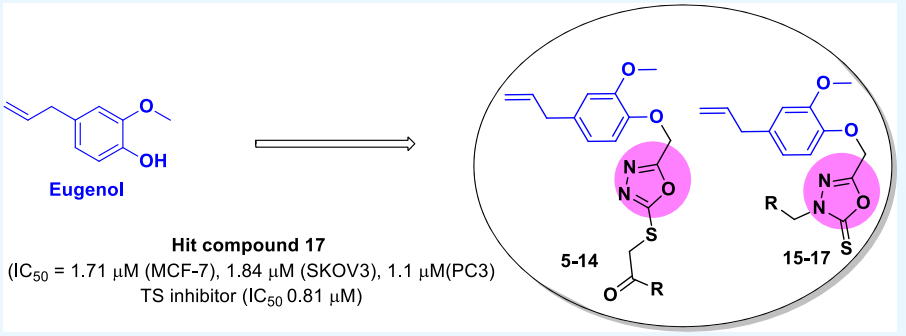

ABSTRACT: Semisynthetic modifications of natural products have bestowed us with many anticancer drugs. In the present work, a natural product, eugenol, has been modified synthetically to generate new anticancer agents. The final compounds were structurally confirmed by NMR, IR, and mass techniques. From the cytotoxicity results, compound **17** bearing morpholine was found to be the most active cytotoxic agent with IC_{50} 1.71 (MCF-7), 1.84 (SKOV3), and 1.1 μM (PC-3) and a thymidylate synthase (TS) inhibitor with an IC_{50} of 0.81 μM. Further cellular studies showed that compound **17** could induce apoptosis and arrest the cell cycle at the S phase in PC-3 carcinoma. The docking study strongly favors compound **17** to be a TS inhibitor as it displayed a similar interaction to 5-fluorouracil. The in silico pharmacokinetics and DFT computational studies support the results obtained from docking and biological evaluation and displayed favorable pharmacokinetic profile for a drug to be orally available. Compound **17** was found to be a promising TS inhibitor which could suppress DNA synthesis and consequently DNA damage in prostate cancer cells.

INTRODUCTION

Natural products are reservoir of bioactive molecules with diverse and remarkable pharmacological potential.[1] Natural products and their semisynthetic molecules have played a fascinating role in the advancement of cancer therapy.[2,3] The semisynthesized natural products derivatives has been an advantage in terms of a better pharmacokinetics profile, diminishing toxicity with improved antiproliferative potential.[4,5] Eugenol (4-allyl-2-methoxyphenol) is a natural aromatic pale yellow phenol with moderate water solubility and complete solubility in organic solvents.[6,7] It possesses important antioxidant, anticancer, antiinflammatory, and antiviral potential.[8,9] It is a nonmalignant and nonmutagenic molecule that exerts anticancer activity through β-catenin/E2F1/surviving downregulation, DNA synthesis inhibition, increased reactive oxygen species production, decreased mitochondrial membrane potential, and triggering apoptosis with cell cycle arrests.[10−13]

Cancer is the second leading cause of deaths globally and increasing tremendously with lung cancer at the top followed by breast and colorectal cancers.[14] The most common treatments employed to fight the disease are chemotherapy, radiotherapy, and surgery while targeted therapies are receiving great attention currently. Among the targets, thymidylate synthase (TS), a folate-dependent enzyme required for DNA replication is attracting medicinal chemists in the field of oncology. This enzyme catalyzes methylation of deoxyuridine monophosphate (dUMP) to thymine monophosphate (dTMP) using CH_2THF cofactor, which after phosphorylation results in thymidine triphosphate (dTTP) formation, a precursor for DNA synthesis.[15] Inhibition of TS causes thymine deprivation resulting in thymidine triphosphate (dTTP) exhaustion, eventually leading to cell death, induction

Received: February 12, 2023
Accepted: May 5, 2023
Published: May 15, 2023

https://doi.org/10.1021/acsomega.3c00933
ACS Omega 2023, 8, 18811−18822

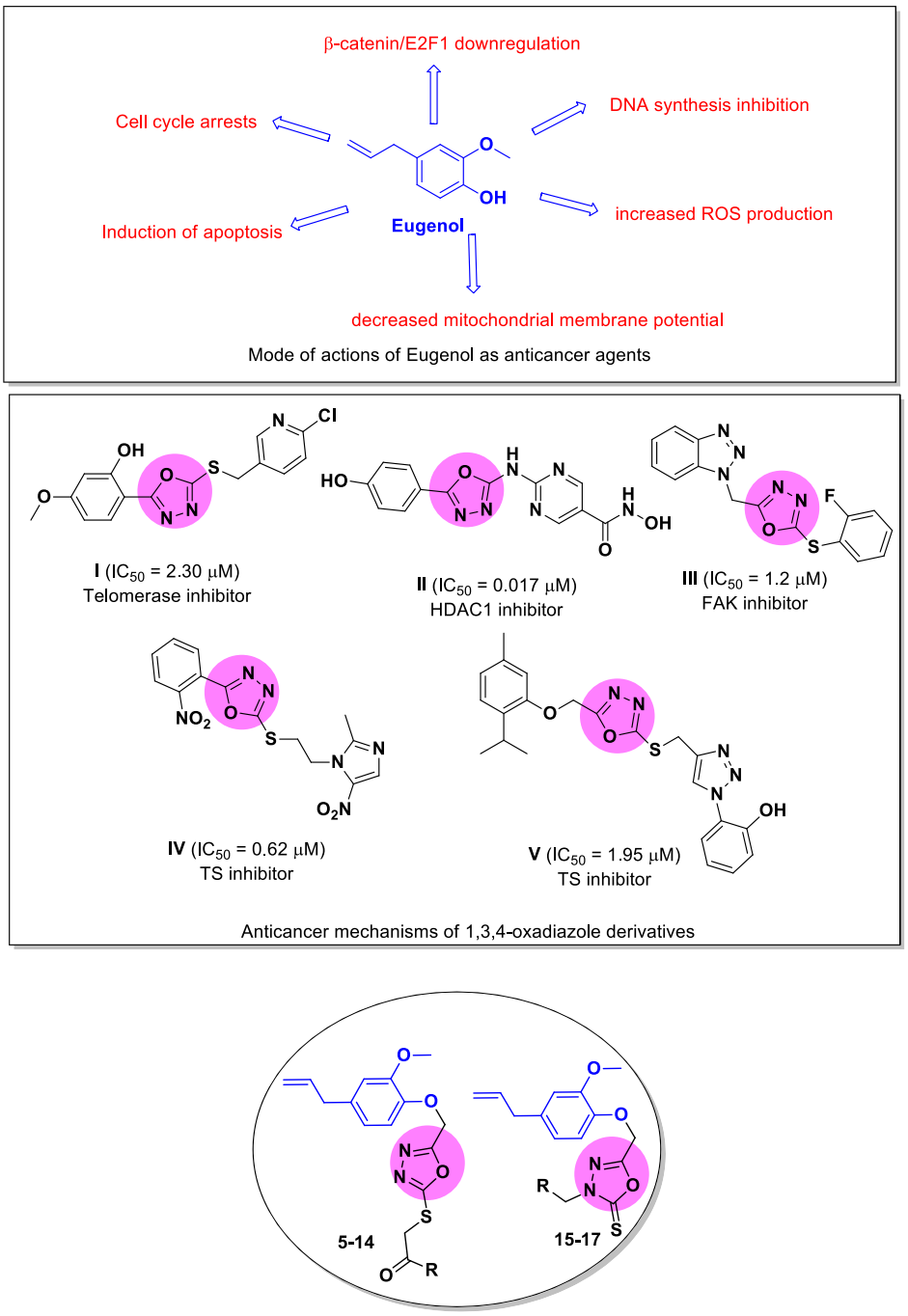

Figure 1. Rationale for the present work.

of apoptosis, and antiproliferation.[16] Also, TS enzyme regulates various proteins involved in the apoptosis process.[17,18] Owing to resistance, insensitivity, and toxicity of the available TS inhibitors,[19,20] new chemotherapeutic agents with better efficacy and safety is an emerging area in the cancer therapy.

During the last decades, the design of 1,3,4-oxadiazole based derivatives as anticancer agents has increased remarkably in medicinal chemistry due to their wide mode of actions.[21] For instance, compound **I** showed a telomerase inhibitory activity with IC_{50} 2.30 μM,[22] compound **II** as HDAC1 inhibitor with IC_{50} = 0.017 μM,[23] compound **III** was found to be 8-fold (IC_{50} 2.1 μM) more effective as FAK inhibitor than Cisplatin (IC_{50} 8.6 μM),[24] while compound **IV** was 15-fold more potent TS inhibitor with IC_{50} 0.62 μM than pemetrexed.[25] Moreover, conjugation of oxadiazole scaffold with bioactive natural products also represents a promising approach.[26−28] Oxadiazole fused thymol (**V**),[29] furanolabdane,[30] and isosteviol derivatives[31] have shown significant inhibitory activities with IC_{50} 1.95 μM, GI_{50} 0.08−0.34 μM, and IC_{50} 0.95−3.36 μM, respectively, toward tested cancer cells (Figure 1). These abovementioned reports of eugenol and 1,3,4-oxadiazole with broad biological targets for antiproliferative effect encouraged us to conjugate natural product eugenol with 1,3,4 oxadiazole scaffold. The present work reports the synthesis of eugenol-based 1,3,4-oxadiazole-hybrids (**5−17**) and their cytotoxicity, docking, and computational studies as TS inhibitors.

https://doi.org/10.1021/acsomega.3c00933
ACS Omega 2023, 8, 18811−18822

Scheme 1. Synthetic Pathway for the Eugenol Derivatives (5−17)

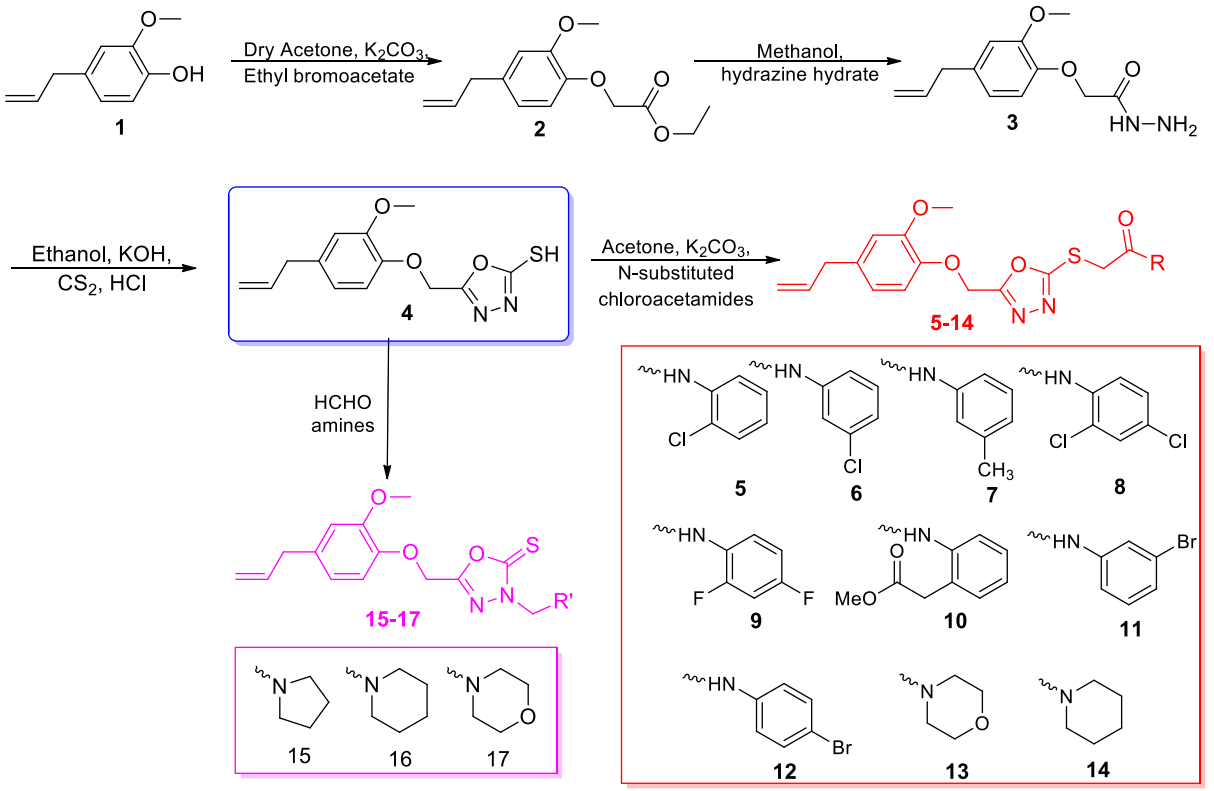

RESULTS AND DISCUSSION

Synthesis and Characterization of Compounds. A natural product, eugenol **1**, was used as the starting material for the synthesis target compounds **5**−**17** (Scheme 1). All the intermediates **2**−**4** were prepared and confirmed by comparing their melting point in the literature.[8] Compound **1** was reacted with ethyl bromo acetate in the presence of potassium carbonate and anhydrous acetone to yield compound **2**, which was treated with hydrazine hydrate in methanol to yield compound **3**. Then, after the addition of carbon disulfide drop by drop in the basic alcoholic mixture of compound **3** at 0−5 °C, the mixture was refluxed for 12 h, and acidification using HCl yielded the key intermediate **4** in 86% yield, which was utilized for the obtainment of final compounds **5**−**17**. Treatment of **4** with freshly prepared different N-substituted chloroacetamides in dry propanone afforded final hybrids **5**−**14** (68−90% yield) and with formaldehyde and different aliphatic amines in ethanol gave compounds **15**−**17** (70−85% yield).

Biological Evaluation. *Antiproliferative Activity.* The final eugenol compounds (**5**−**17**) were screened for antiproliferative activity against three human adenocarcinomas, namely, breast (MCF-7), prostate (PC-3), and ovarian (SKOV3) using the MTT method as previously described.[32] The results are illustrated in Table 1. Among all the final compounds, 1,3,4-oxadiazole-Mannich base bearing morpholine heterocycle (**17**) was the most active cytotoxic agent with IC_{50} 1.71, 1.84, and 1.1 μM, while doxorubicin exhibited IC_{50} 1.74, 2.88, and 2.61 μM, against MCF-7, SKOV3, and PC-3, respectively. Also, compound **9** having fluoro-substituted thioacetamide group exhibited promising cytotoxicity with IC_{50} in the range 2.09−3.36 μM toward the tested cell lines. Against the breast cancer cells, compounds **8**, **12**, and **15** displayed significant cytotoxicity with IC_{50} < 10 μM, compounds **5**, **6**, and **11** were moderately cytotoxic with IC_{50} less than 25 μM and other compounds were found to be mild and inactive. Against ovarian and prostate cancer cells, compound **10** with the COOMe group displayed good sensitivity with IC_{50} 8.74 and 7.07 μM, respectively; however, it was mildly cytotoxic against breast cancer cells. Besides, compound **15** possessing pyrrolidine ring in the Mannich base skeleton displayed good antiproliferation toward prostate carcinoma with IC_{50} 10.01 μM. Compounds **5**, **11**, **12**, **15**, and **16** with IC_{50} in the range 14.09−26.33 μM and

Table 1. In Vitro Cytotoxicity of Eugenol Derivatives (5−17)[a]

	half maximal inhibitory concentration (IC_{50}, μM)		
compounds	breast MCF7	ovarian SKOV3	prostate PC3
5	25.74 ± 3.52	15.73 ± 3.43	11.18 ± 2.72
6	16.33 ± 2.80	41.06 ± 5.27	16.98± 1.08
7	45.89 ± 3.80	65.4 ± 2.81	24.30 ± 1.53
8	10.74 ± 2.76	70.01 ± 2.42	29.96 ± 0.91
9	**2.87±0.56**	**3.36±0.80**	**2.09±0.68**
10	45.01 ± 2.92	8.74 ± 1.06	7.07 ± 3.90
11	15.21 ± 3.77	26.33 ± 3.09	51.09 ± 2.92
12	6.54 ± 1.42	14.09 ± 2.17	16.72 ± 4.10
13	38.92 ± 3.20	61.09 ± 3.84	20.27 ± 0.75
14	172.86 ± 1.36	181.46 ± 3.58	124.90 ± 0.36
15	9.55 ± 0.71	16.86 ± 1.64	10.01 ± 0.99
16	33.18 ± 2.04	19.54 ± 2.48	26.65 ± 0.86
17	**1.71±0.95**	**1.84±0.27**	**1.1±0.07**
doxorubicin	1.74 ± 0.34	2.88 ± 0.68	2.61 ± 0.23

[a]Data represent the mean values ± standard deviation of three independent experiments.

https://doi.org/10.1021/acsomega.3c00933
ACS Omega 2023, 8, 18811−18822

compounds **5**, **6**, **7**, **8**, **12**, **13**, and **16** with IC_{50} in the range 11.18−29.96 μM were found to be moderate in killing the ovarian and prostate cancer cells, respectively. The remaining compounds were either mild (IC_{50} > 50) or less active (IC_{50} > 100). From these data, it is clear that most of the eugenol derivatives (except **14**) have the ability to hinder cancer cell proliferation.

In Vitro Thymidylate Synthase Activity. The cytotoxic hybrids (**8**, **9**, **10**, **12**, **15**, and **17**) with $IC_{50} \leq 10$ μM against the tested cell lines, were selected for the TS inhibition activity in order to recognize their mechanism as TS inhibitors. These compounds as shown in Table 2 significantly inhibited TS with IC_{50} 1.01, 1.21, and 0.81 μM for compounds **9**, **10**, and **17**, respectively, which supports the promising cytotoxicity of these compounds whereas pemetrexed inhibited TS with IC_{50} 2.81 μM. Other compounds **12** and **15** displayed comparable TS repression to pemetrexed, while compound **8** was found to be a moderate TS inhibitor. These data suggest that the synthesized eugenol derivatives have the potential to suppress TS enzyme leading to cancer cell antiproliferation.

Table 2. In Vitro TS Activity[a]

compounds	IC_{50} (μM)
8	3.67 ± 0.58
9	**1.01±0.41**
10	1.25 ± 0.35
12	2.93 ± 0.71
15	2.57 ± 0.31
17	**0.81±0.21**
pemetrexed	2.81 ± 0.31

[a]IC_{50} values are the mean ± S.D. of three separate experiments.

Compound 17 Arrest Cell Cycle at S Phase. Cell cycle dysregulation is an important cause of cancer cells proliferation, therefore blocking the cell cycle is an effective strategy to prevent cell proliferation. Compound **17**, the most potent cytotoxic compound on PC-3 cells and elicited highest TS inhibitory activity was selected to explore its cellular mechanism responsible for cancer cell antiproliferation. Exposure of PC-3 cells with compound **17** and the control were stained with propidium iodide at their pre calculated, IC_{50} for 48 h and their effects on cell cycle profile and apoptosis were analyzed by flow cytometry.[33] As illustrated in Figure 2, compound **17** increased the percentage of cell population at the S phase of the cell cycle from 37.69 to 62.07%, compared to vehicle control. Such increase was accompanied by the significant reduction of cell population at G1 and G2 phases from 37.69 to 29.30 and 24.60 to 8.61%, respectively. These results suggested that compound **17** could arrest cell cycle at the S phase.

Compound 17 Induced Cancer Cell Apoptosis in PC-3 Cells. To further assure the apoptotic ability of compound **17**, a flow cytometric assay utilizing Annexin V-propidium iodide dual staining was performed, which differentiates between live, apoptotic (early and late), and necrotic cells. As shown in Figure 3, after 48 h of treatment of PC-3 cells with compound **17**, a decrease in the percentage of live cells in green (R1) were noticed. Moreover, a significant increase in total apoptotic (early and late in purple and blue) cells was observed from 1.08 to 47.58% (R2 and R4) as a slight increase in necrotic cells to 3.56% (R1, red color) from 1.62%. This result indicates that compound **17** induces apoptosis in PC-3 cells.

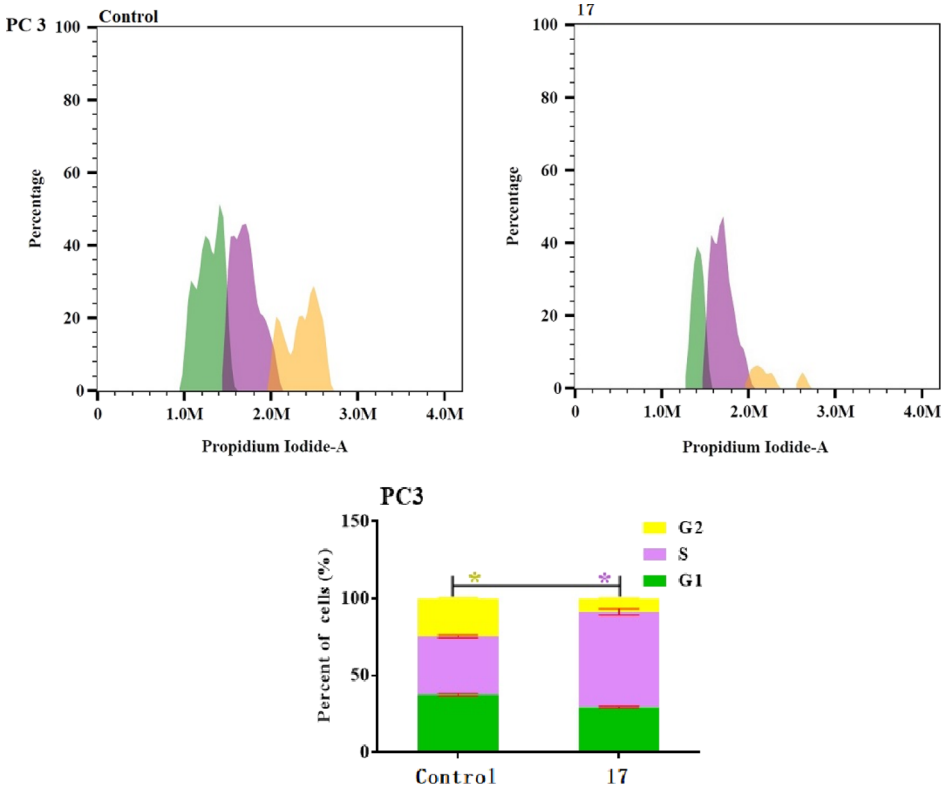

Figure 2. Cell cycle distribution of compound **17** and control at their pre calculated IC_{50} for 48 h in prostate PC3 cells by PI staining using flow cytometry. One-way ANOVA was used to test for statistical difference (*p < 0.05).

https://doi.org/10.1021/acsomega.3c00933
ACS Omega 2023, 8, 18811−18822

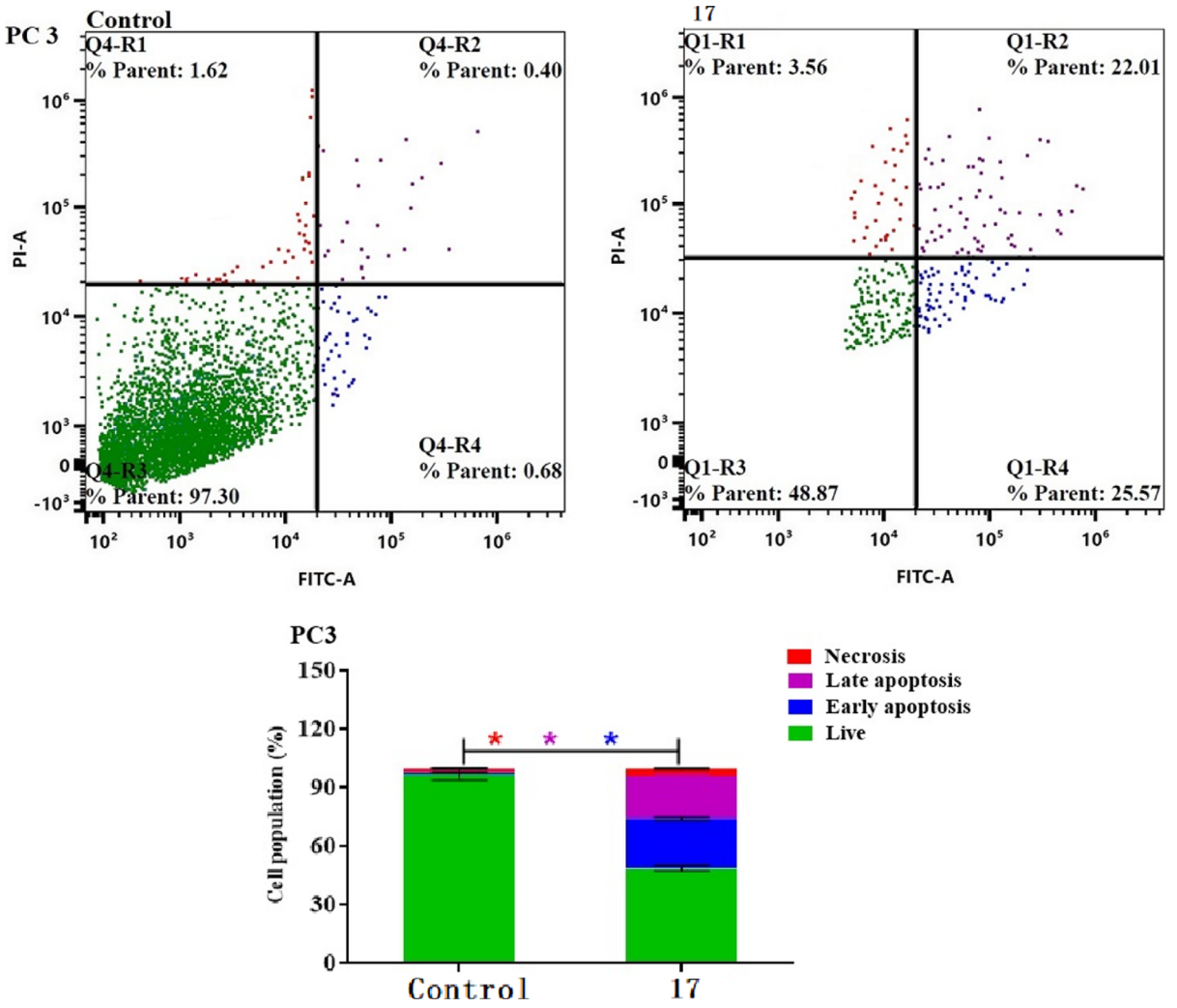

Figure 3. Apoptosis analysis of compound **17** and control at their pre calculated IC_{50} for 48 h in prostate PC3 cells by PI staining using flow cytometry. One-way ANOVA was used to test for statistical difference ($*p < 0.05$).

Table 3. In Silico Physicochemical/Pharmacokinetic Properties of Eugenol Hybrids (5−17)[d]

	Lipinski parameters									
compd. no.	MW[a]	HBA[b]	HBD[c]	*i* log $P_{o/w}$	violations	nROTB[e]	TPSA[f]	% ABS[g]	BBB[h]	GI ABS[i]
5	445.92	6	1	4.23	0	10	111.78	70.43	no	high
6	445.92	6	1	3.53	0	10	111.78	70.43	no	high
7	425.50	6	1	3.55	0	10	111.78	70.43	no	high
8	480.36	6	1	4.45	0	10	111.78	70.43	no	high
9	447.46	8	1	3.95	0	10	111.78	70.43	no	high
10	469.51	8	1	4.17	0	11	138.08	61.36	no	low
11	490.37	6	1	3.12	0	10	111.78	70.43	no	high
12	490.37	6	1	3.20	0	10	111.78	70.43	no	high
13	405.47	7	0	3.62	0	9	112.22	70.28	no	high
14	403.50	6	0	3.95	0	9	102.99	73.46	no	high
15	361.46	5	0	3.97	0	8	84.75	79.76	no	high
16	375.49	5	0	4.16	0	8	84.75	79.76	no	high
17	377.46	6	0	3.97	0	8	93.98	76.57	no	high

[a]Molecular weight. [b]Hydrogen bond acceptor. [c]Hydrogen bond donor. [d]Partition coefficient. [e]Number of rotable bonds. [f]Topological PSA. [g]Absorption %. [h]Blood−brain barrier. [i]Gastrointestinal absorption.

The outcomes of cell cycle and apoptosis studies were found to be in agreement with the reported literature.[34,35] 5-fluorouracil and other TS inhibitors arrest the S stage of the cycle in different cancer cells. In the present work also, compound **17** displayed significant TS suppression via arresting S stage and apoptosis, indicating that compound **17** could block thymidine triphosphate (dTTP) leading to controlled antiproliferation.

https://doi.org/10.1021/acsomega.3c00933
ACS Omega 2023, 8, 18811−18822

Table 4. Toxicity Studies of the Eugenol Hybrids (5−17)

compds	AMES toxicity	LD_{50} (mol/kg)	oral rat chronic toxicity (log mg/kg b.w/day)	hepatotoxicity	skin sensitization
5	no	2.52	0.987	yes	no
6	no	2.52	0.987	yes	no
7	no	2.46	1.21	yes	no
8	no	2.63	0.785	yes	no
9	no	2.50	0.916	yes	no
10	no	2.46	1.04	yes	no
11	no	2.54	0.977	yes	no
12	no	2.54	0.977	yes	no
13	no	2.71	1.834	yes	no
14	no	2.88	1.294	yes	no
15	no	2.79	1.08	yes	no
16	no	2.82	1.007	yes	no
17	no	2.622	1.273	yes	no

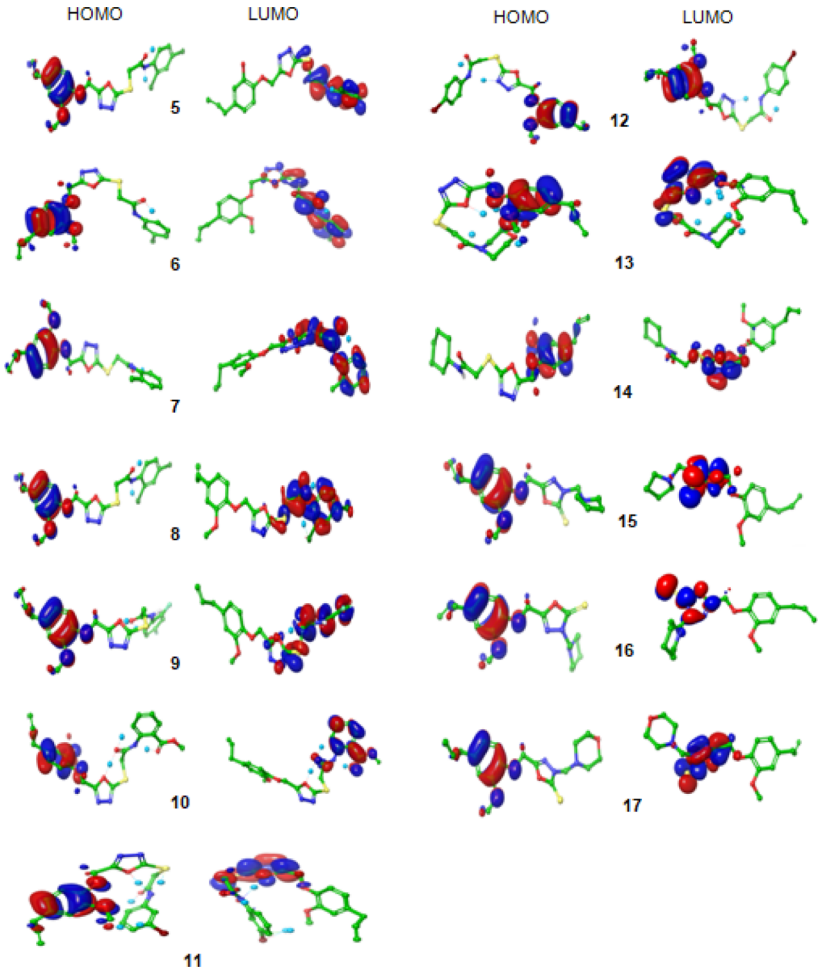

Figure 4. HOMO and LUMO molecular orbital for compounds **5**−**17**.

In Silico Physicochemical and Pharmacokinetics Studies. The development of new drugs has been a costly, risky and challenging venture with a low victory success rate. Most of the molecules, due to undesirable drawbacks and low efficacy in clinical trials do not reach the market. Therefore, in silico pharmacokinetic and toxicity prediction in early stages of drug development provides an idea about the effectiveness and success of the molecule therapeutically. The emergence of computational studies has led to optimization of pharmacokinetic and toxicity parameters resulting in drug discovery in an efficient manner. The physicochemical and pharmacokinetic properties of the newly synthesized hybrids (**5**−**17**) have been evaluated by Swiss ADME software.[36] The fate of the synthesized molecules for successful drug depends upon certain rules such as Lipinski and Veber. Lipinski rules are hall mark in the innovation and discovery of a drug which states that a molecule must have MW < 500, lipophilicity (i log $P_{o/w}$) < 5, hydrogen bond acceptor (HBA) below 10 and hydrogen bond donor (HBD) below 5. These rules further included molecule flexibility (nROTB) and polar surface area (PSA) less than 10 and 140 $Å^2$, respectively. It can be observed from Table 3 that the synthesized molecules possess promising

https://doi.org/10.1021/acsomega.3c00933
ACS Omega 2023, 8, 18811−18822

Table 5. DFT Calculations of Eugenol Derivatives 5−17 Computed by the B3LYP and 6-311G** (d,p) Basis Set

no.	E_{HOMO} (eV)	E_{LOMO} (eV)	E_g (eV)	H (eV)	S (eV)	χ (eV)	IP (eV)	ω (eV)
5	−5.959	−1.061	4.898	2.449	302.318	−3.510	3.510	2.503
6	−6.095	−1.524	4.572	2.286	323.815	−3.810	3.810	3.175
7	−5.905	−1.225	4.680	2.340	316.196	−3.565	3.565	2.715
8	−8.003	−0.767	7.236	3.618	204.650	−0.017	0.017	0.000
9	−5.905	−1.687	4.218	2.109	351.114	−3.796	3.796	3.416
10	−5.905	−0.871	5.034	2.517	294.176	−3.388	3.388	2.280
11	−5.823	−2.068	3.755	1.878	394.367	−3.946	3.946	4.146
12	−5.986	−1.497	4.490	2.245	329.834	−3.742	3.742	3.118
13	−5.769	−1.551	4.218	2.209	351.114	−3.660	3.660	3.176
14	−5.986	−1.551	4.435	2.218	333.881	−3.769	3.769	3.202
15	−5.959	−1.279	4.680	2.340	316.411	−3.619	3.619	2.798
16	−5.905	−0.980	4.925	2.463	300.678	−3.442	3.442	2.406
17	−5.905	−0.980	4.925	2.463	300.678	−3.442	3.442	2.406

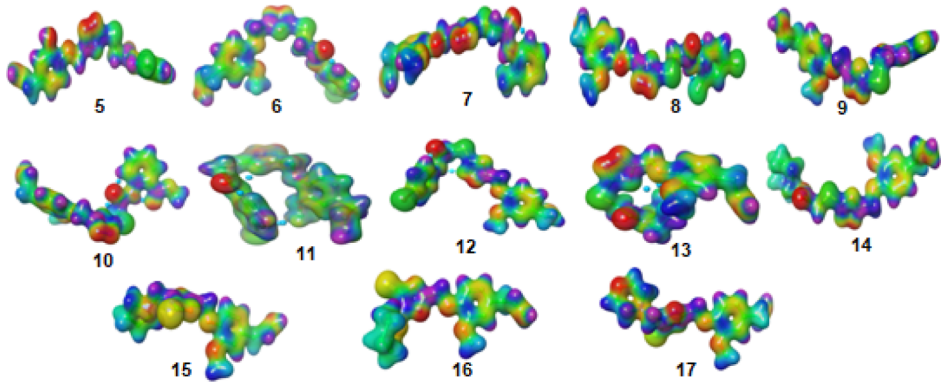

Figure 5. MEP for the eugenol derivatives (**5**−**17**).

oral absorption and permeability as they did not show any Lipinski violations in respect of molecular weight, HBA, HBD, and lipophilicity. Also all the compounds except **10** were found to be flexible, suggesting that they did not have bioavailability problem. All the compounds possess high gastrointestinal absorption in the range 70.43−79.76%, except compound **10** which displayed low gastrointestinal absorption of 61.36%. All the molecules were found to be nonpermeable to the brain. These results suggested that the synthesized molecules have acceptable physicochemical and pharmacokinetics features, which are required for a molecule to be orally available.

The toxicity prediction of the synthesized hybrids (**5**−**17**) was done by available software tools (http://biosig.unimelb.edu.au/pkcsm/prediction) and is shown in Table 4. All the molecules were found to be non-mutagenic, noncarcinogenic, and safe with LD_{50} in the acceptable range of 2.46−2.82 mol/kg. Chronic toxicity was also found to be in the safer zone with no skin sensitization effect. However, these compounds were found to be hepatotoxic.

DFT Physicochemical Properties. The quantum theory approximation is one of the reliable computational methods in drug discovery. DFT/B3LYP/6-311G**(d,p) with TD-DFT measurements were done for eugenol derivatives **5**−**17**. The difference between the charge separation in HOMO and LUMO of the molecules designates Fermi molecular orbitals, as depicted in Figure 4.

The electronic envelop was cumulated on the donor fragment, 4-allyl-1,2-dimethoxyphenyl fragments in HOMO orbital which was switched to LUMO orbital characterized by thiomethyl triazole and the substituted aromatic moieties for compounds **1**−**10**, **13**, **14**, thiomethyl triazole and oxadiazole ring in compounds **11**, **15**−**17**; however, in compound **12**, localization of the LUMO zone was distributed in similar manner to HOMO. DFT calculations were applied to calculate HOMO, LUMO, and energy gap (E_g) illustrated in Table 5.

It was found that strong relationship exists between E_g and nature of the substituents such as 2−Cl−C_6H_5; 3−Cl−C_6H_5; 2−CH_3−C_6H_5; 2,4-dichlore−C_6H_4; 2,4-difoloro−C_6H_4; morpholineyl; C_6H_{11}; 2−COOH−C_6H_4−; 2−Br−OCH_3−C_6H_4; 4−Br−C_6H_4; pyrrolidinyl; and piperidinyl and morpholinomethyl and the E_g was found in the order, 3.755 (**11**) < 4.218 (**9**, **13**) < 4.435 (**14**) < 4.490 (**12**) < 4.572 (**6**) < 4.680 (**7**, **15**) < 4.898 (**5**) < 4.925 (**16**) < 4.925 (**17**) < 5.034 (**10**) < 7.23 (**8**). For chemical reactivity, parameters such as electronegativity (χ), chemical potential (IP), and electrophilicity index (ω) were calculated which correspond to more electrophilic (HOMO) and nucleophilic (LUMO) sites. The antioxidant potential of the molecules is inversely proportional to ionization potential,[16] and we observed that all the synthesized eugenol derivatives possess low IP indicating that these molecules have good potential to scavenge free radicals.

Molecular Potential Maps. The presence of electron density and chemical reactivity of synthesized molecules toward nucleophilic or electrophilic sites of biological media can be distinguished by molecular electrostatic potential (MEP). The MEP of the synthesized molecules was generated by the same DFT parameters as discussed before. As shown in Figure 5, the red color signifies the electrophilic zone with negative potential, blue color as the nucleophilic zone and positive potential, while the green zone for a neutral site. It can

https://doi.org/10.1021/acsomega.3c00933
ACS Omega 2023, 8, 18811−18822

be observed that the negative potential (red surfaces) surrounds the oxadiazole ring and positive potential (blue surfaces) was distributed around the molecular skeletons. These zones in MEPs were responsible in detection of the active site for the receptors.

Molecular Docking Study. The synthesized eugenol derivatives (**5**−**17**) were docked against TS protein (PDB 6QXG) to support out biological results. It has been reported that 5-fluorouracil (5-FU) interacts with the active site through GLY222, SER216, ASN226, ARG50, HIS256, ARG175, CYS195, GLY217, ASP218, ARG215, and ARG176 residues.[30] The induce-fit-docking was applied to generate final poses by OPLS force field. The final pose was selected based on both lowest binding free energy (Δ*G*) and RMSD. The inhibition-constant (Ki) was generated for all the compounds **5**−**17**, which must be in the range 0.1−1.0 μM, and inversely proportional to binding energy efficiency (Table 6). Our docking findings revealed that the compounds **5**−**17** can perceive the key amino acids in diverse ways such as hydrogen bonding, arene cations, and arene−arene interactions.

Table 6. Binding-Affinity Energies (kcal/mol) of Eugenol Derivatives (5−17) against TS[a]

no.	ΔG	RMSD	H. B	EInt.	Eele	Ki
5FU	−8.10	2.19	435.10	−16.66	−12.39	0.94
5	−7.52	1.53	26.24	−17.01	−7.86	1.98
6	−7.48	1.84	6.83	−16.56	−8.75	1.54
7	−7.56	3.52	13.84	−13.42	−8.03	2.16
8	−7.68	2.61	21.41	−16.67	−7.21	1.73
9	−7.75	1.71	38.28	−16.21	−7.32	1.94
10	−7.82	3.69	37.42	−6.71	−7.25	1.81
11	−7.59	2.16	17.01	−13.90	−8.19	1.43
12	−7.76	2.66	13.18	−12.18	−9.71	1.49
13	−7.52	2.87	65.71	−14.14	−8.31	1.56
14	−7.74	1.69	10.64	−16.29	−7.34	0.16
15	−7.20	1.38	57.63	−16.47	−9.53	0.94
16	−6.90	2.41	53.95	−9.61	−8.42	1.02
17	−7.89	4.26	95.13	−10.23	−7.41	1.98

[a]Where ΔG: free binding energy of the ligand; RMSD: root-mean-square deviation; H.·B: H-bonding energy between protein and ligand; EInt.: binding affinity of H-bond interaction with receptor; and Eele: electrostatic interaction over the receptor.

As shown in Table 6 and Figure 6, all the compounds except 16 have nearly the same binding energy (Δ*G* in the range −7.20 to −7.89 kcal/mol), but lower than reference drug, 5-FU (Δ*G* −8.10 kcal/mol), and displayed interactions with the active site similar to 5FU, suggestion that the synthesized molecules interacted with TS protein analogues to 5FU as TS inhibitor. The most active compounds **9** and **17** were found to bind with the TS pocket via H-bond with Arg50 amino acid. Furthermore, compound 9 also formed other H-bond with Arg176 and π−π interaction with Trp109, whereas C═S of compound 17 formed strong H-bond with Arg50, Arg175, and π−π interaction with Arg215. Other compounds were stabilized in binding pocket of the vital TS backbone through binding with ASN226, CYS195, ASP218, ARG50, ARG175, ARG215, SER216, and ARG176. The docking interaction of compounds **9** and **17** strongly support their in vitro TS inhibitory activity with IC_{50} 1.01 and 0.81 μM, respectively. From the above results, compound **17** emerged as a promising lead for a TS inhibitor.

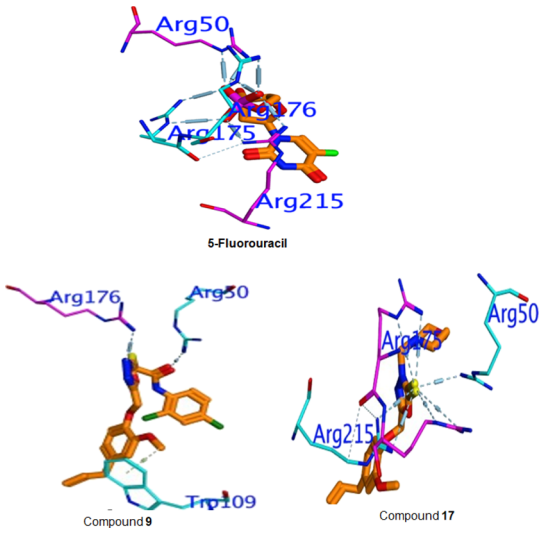

Figure 6. Docking poses of compounds **9**, **17**, and 5-FU

CONCLUSIONS

Eugenol-based new 1,3,4-oxadiazole incorporated N-substituted acetamide and Mannich bases as anticancer agents were prepared with moderate to good yield. In silico physicochemical and toxicity studies of the molecules showed that most of the molecules have drug likeness properties and found to be non-mutagenic, noncarcinogenic, and safe with LD_{50} in the acceptable range of 2.46−2.82 mol/kg. Cytotoxicity results concluded that compound 17 bearing a morpholine ring was found to be the most active which blocks proliferation of breast, ovarian, and prostate cancer cells with IC_{50} 1.71, 1.84, and 1.1 μM, respectively, and TS inhibition effectively with IC_{50} of 0.81 μM. It induces S phase arrest due to S phase checkpoint activation and triggers apoptosis by irreparable DNA damage in PC3 cells.

EXPERIMENTAL SECTION

Materials and Methods. The solvents and other reagents required for the synthesis of target molecules were either purchased from Sigma-Aldrich (Merck Germany), Across (USA) or freshly prepared in the lab. NMR spectra, FT-IR, and mass spectra were recorded on a Bruker spectrometer in $CDCl_3$ at 80 MHz, Thermo Scientific spectrophotometer (ATR method), and Thermo Scientific LCQ Fleet (LCF10605), respectively, while melting points were performed on a SMP40 machine which were uncorrected. Target molecules were analyzed for their elemental composition on LEECO Elementar Analyzer. Compounds **2**−**4** were prepared according to our previous reported work.[8]

General Procedure for Synthesis of Compounds 5−14. Compound **4** (2 mmol), anhydrous acetone (50 mL), and potassium carbonate (1.5 mmol) were refluxed for an hour and then cooled to 40−45 °C and added by different N-substituted chloroacetamides (1.1 mmol). Refluxing was continued for 6−12 h, while reaction monitoring was carried out by TLC silica gel 60 $WF_{254}S$ aluminum sheet. After consumption of the starting reactants, it was filtered, and the filtrate was concentrated and poured in water (50 mL) and extracted with ethyl acetate (50 mL). Recrystallization was employed to purify the compounds using petroleum ether/ethyl acetate or isopropyl alcohol or dichloromethane/cyclohexane.

https://doi.org/10.1021/acsomega.3c00933
ACS Omega 2023, 8, 18811−18822

*2-((5-((4-Allyl-2-methoxyphenoxy)methyl)-1,3,4-oxadiazol-2-yl)thio)-N-(2-chlorophenyl) Acetamide (**5**).* Recryst. solvent: petroleum ether-ethylacetate; yield: 82%; mp 90−92 °C; FT-IR (cm^{-1}): 2927.47, 1699, 1607, 1588, 1510, 1367, 1248, 1139, 1027, 753; ^{1}H NMR: 3.36 (d, J = 6.4 Hz, 2H, Ar−CH_2−), 3.89 (s, 3H, Ar−O−CH_3), 4.08 (s, 2H, −S−CH_2−), 4.61 (s, 2H, −O−CH_2−), 5.00−5.25 (m, 2H, CH_2═CH−), 5.73−6.23 (m, 1H, CH_2═CH−), 6.66−6.83 (m, 3H, Ar−H), 7.40−7.50 (m, 4H, Ar−H), 9.14 (s, 1H, Ar−N−H); ^{13}C NMR: 32.98 (S−CH_2−), 39.84 (−CH_2−Ar), 55.85 (Ar−O−CH_3), 69.97 (Ar−O−CH_2−), 112.54, 116.02, 120.96, 128.16, 130.48, 131.13, 132.45, 135.58, 137.25, 145.53, 149.68, 158.29, 164.56, 169.76 (−C═O). ESI (+ve): 446.50 $[M + H]^+$. Elemental analyses for $C_{21}H_{20}ClN_3O_4S$ (calcd): C, 56.56; H, 4.52; N, 9.42; S, 7.19. Found: 56.44; H, 4.54; N, 9.47; S, 7.17.

*2-((5-((4-Allyl-2-methoxyphenoxy)methyl)-1,3,4-oxadiazol-2-yl)thio)-N-(3-chlorophenyl) Acetamide (**6**).* Recryst. solvent: petroleum ether-ethylacetate; yield: 69%, mp 88−90 °C, FT-IR (cm^{-1}): 3287, 3009, 2929, 1673, 1596, 1535, 1510, 1480, 1458, 1418, 1392, 1282, 1247, 1220, 1161, 1024, 824, 803, 749, 731. ^{1}H NMR: 3.34 (d, J = 6.4 Hz, 2H, Ar−CH_2−), 3.84 (s, 3H, Ar−O−CH_3), 4.09 (s, 2H, S−CH_2−), 4.99−5.25 (m, 4H, CH_2═CH−, O−CH_2−), 5.72−6.13 (m, 1H, CH_2═CH−), 6.64−7.01 (m, 6H, Ar−H), 8.25−8.36 (m, 1H, Ar−H), 9.14 (s, 1H, Ar−NH−); ^{13}C NMR: 36.50 (S−CH_2−), 39.92 (−CH_2−Ar), 55.85 (Ar−OCH_3), 61.81 (Ar−O−CH_2−oxadiazole), 110.20, 112.78, 116.04, 116.66, 120.08, 120.70, 121.03, 124.43, 127.44, 135.94, 137.31, 144.52, 148.42, 164.93, 175.05 (C═O). ESI (+ve): 446.33 $[M + H]^+$. Elemental analyses for $C_{21}H_{20}ClN_3O_4S$ (calcd): C, 56.56; H, 4.52; N, 9.42; S, 7.19. Found: C, 56.48; H, 4.54; N, 9.39; S, 7.14.

*2-((5-((4-Allyl-2-methoxyphenoxy)methyl)-1,3,4-oxadiazol-2-yl)thio)-N-(m-tolyl)acetamide (**7**).* Recryst. solvent: dichloromethane-cyclohexane; yield: 69%, mp 72−74 °C, ^{1}H NMR: 2.29 (s, 3H, Ar−CH_3), 3.38 (d, J = 6.4 Hz, Ar−CH_2−), 3.90 (s, 3H, Ar−O−CH_3), 4.09 (s, 2H, S−CH_2), 4.63 (s, 2H, O−CH_2−), 5.03−5.19 (m, 2H, CH_2═CH−), 5.75−6.14 (m, 1H, CH_2═CH−), 6.79−6.85 (m, 3H, Ar−H), 7.31−7.37 (m, 4H, Ar−H), 9.13 (s, 1H, Ar−NH−); ^{13}C NMR: 17.71, 33.02, 39.91, 55.91, 69.92, 112.65, 115.93, 116.09, 121.01, 127.36, 128.35, 130.06, 131.55, 135.62, 137.33, 145.55, 149.72, 164.61, 170.37. ESI (+ve): 426.33 [M + H]+; elemental analyses for $C_{22}H_{23}N_3O_4S$ (calcd): C, 62.10; H, 5.45; N, 9.88; S, 7.54. Found: C, 62.21; H, 5.48; N, 9.85; S, 7.56.

*2-((5-((4-Allyl-2-methoxyphenoxy)methyl)-1,3,4-oxadiazol-2-yl)thio)-N-(2,4-di-chlorophenyl) Acetamide (**8**).* Recryst. solvent: isopropyl alcohol; yield: 84%, mp 96−98 °C, FT-IR (cm^{-1}): 3264, 3064, 1689, 1645, 1596, 1506, 1481, 1211, 829, 800. ^{1}H NMR: 3.33 (d, J = 6.4 Hz, 2H, Ar−CH_2−), 3.87 (s, 3H, Ar−O−CH_3), 4.07 (s, 2H, S−CH_2−), 4.59 (s, 2H, −O−CH_2−), 4.99−5.14 (m, 2H, CH_2═CH−), 5.71−6.00 (m, 1H, CH_2═CH═), 6.75 (brd, s, 3H, Ar−H), 7.35−7.54 (m, 3H, Ar−H), 9.15 (s, 1H, Ar−N−H); ^{13}C NMR: 32.98, 39.93, 55.91, 70.08, 112.55, 116.09, 121.05, 128.65, 130.56, 131.35, 133.48, 137.27, 145.57, 150.69, 155.00, 161.37, 164.59, 169.51. ESI (+ve): 481.17 [M + H]+; 483.17 [M + 2 + H]+; elemental analyses for $C_{21}H_{19}Cl_2N_3O_4S$ (calcd): C, 52.15; H, 3.99; N, 8.75; S, 6.68. Found: C, 52.26; H, 4.02; N, 8.77; S, 6.65.

*2-((5-((4-Allyl-2-methoxyphenoxy)methyl)-1,3,4-oxadiazol-2-yl)thio)-N-(2,4-diflorophenyl) Acetamide (**9**).* Recryst. solvent: petroleum ether-ethylacetate; yield: 72%, mp 124−128 °C, FT-IR (cm^{-1}): 3341, 3063, 1689, 1505, 1446, 1399, 1293, 1210, 830, 800. ^{1}H NMR: 3.41 (brs, 2H, Ar−CH_2−), 3.92 (s, 3H, Ar−O−CH_3), 6.72−7.33 (m, 6H, Ar−H), 8.82 (s, 1H, Ar−N−H); ^{13}C NMR: 32.98, 38.07, 54.34, 63.74, 112.79, 114.74, 116.84, 121.16, 122.44, 127.43, 128.90, 130.15, 141.85, 145.03, 154.70, 158.53, 163.37. ESI (−ve): 446.08 [M − H]+; elemental analyses for $C_{21}H_{19}F_2N_3O_4S$ (calcd): C, 56.37; H, 4.28; N, 9.39; S, 7.17. Found: C, 56.45; H, 4.30; N, 9.36; S, 7.15.

*Methyl-2-(2-((5-((4-allyl-2-methoxyphenoxy)methyl)-1,3,4-oxadiazol-2-yl)thio)acetamido) Benzoate (**10**).* Recryst. solvent: petroleum ether-ethylacetate; yield: 74%, mp 86−88 °C, FT-IR (cm^{-1}): 3285, 2981, 1683, 1646, 1590, 1506, 1487, 1229, 1154, 996, 788; ^{1}H NMR: 3.36 (d, J = 6.4 Hz, Ar−CH_2−), 3.87−3.94 (m, 6H, Ar−O−CH_3), 4.24 (s, 2H, S−CH_2−), 5.02−5.27 (m, 4H, CH_2═CH−, O−CH_2−), 5.83−6.04 (m, 1H, CH_2═CH−), 6.66−7.31 (m, 5H, Ar−H), 7.59 (t, J = 6.4 Hz, 1H), 8.50 (d, J = 8.0 Hz, 1H), 8.64 (s, 1H, ArNH); ^{13}C NMR: 37.24, 39.81, 52.45, 55.79, 61.69, 112.65, 115.91, 116.52, 120.61, 123.27, 130.84, 134.57, 137.23, 140.57, 145.09, 150.15, 164.91, 168.24. ESI (+ve): 470.25 [M + H]+; elemental analyses for $C_{23}H_{23}N_3O_6S$ (calcd): C, 58.84; H, 4.94; N, 8.95; S, 6.83. Found: C, 58.75; H, 4.96; N, 8.99; S, 6.85.

*2-((5-((4-Allyl-2-methoxyphenoxy)methyl)-1,3,4-oxadiazol-2-yl)thio)-N-(3-bromophenyl) Acetamide (**11**).* Recryst. solvent: isopropyl alcohol; yield: 64%, mp 114−116 °C; FT-IR (cm^{-1}): 3185, 2987, 1730, 1673, 1607, 1592, 1509, 1374, 1250, 1141, 1026, 965, 965, 800; ^{1}H NMR: 3.33 (d, J = 6.4 Hz, Ar−CH_2−), 3.83 (s, 3H, Ar−O−CH_3), 4.03 (s, 2H, S−CH_2−), 4.62−5.14 (m, 4H, CH_2═CH−, O−CH_2−), 5.71−5.97 (m, 1H, CH_2═CH−), 6.57−6.81 (m, 3H, Ar−H), 7.18−7.79 (m, 4H, Ar−H), 9.5 (s, 1H, Ar−NH−); ^{13}C NMR: 32.98 (S−CH_2−), 39.83 (−CH_2−Ar), 55.77 (Ar−OCH_3), 61.45 (Ar−O−CH_2−oxadiazole), 112.57, 115.87, 116.01, 120.97, 122.64, 126.63, 130.66, 130.94, 132.94, 135.60, 137.39, 145.11, 145.43, 149.02, 164.75. ESI (+ve): 490 [M + H]+; 492 [M + 2 + H]+; elemental analyses for $C_{21}H_{20}BrN_3O_4S$ (calcd): C, 51.44; H, 4.11; N, 8.57; S, 6.54. Found: C, 51.51; H, 4.12; N, 8.54; S, 6.53.

*2-((5-((4-Allyl-2-methoxyphenoxy)methyl)-1,3,4-oxadiazol-2-yl)thio)-N-(4-bromophenyl) Acetamide (**12**).* Recryst. solvent: isopropyl alcohol; yield: 90%, mp 128−130 °C; FT-IR (cm^{-1}):3188, 2985, 2930, 1729, 1670, 1602, 1509, 1488, 1375, 1251, 1208, 1141, 1030, 964, 913, 798; ^{1}H NMR: 3.42 (d, J = 6.4 Hz, 2H, Ar−CH_2−), 3.95 (s, 3H, Ar−O−CH_3), 4.12 (s, 2H, S−CH_2−), 4.69 (s, 2H, O−CH_2−), 5.07−5.31 (m, 2H, CH_2═CH−), 5.86−6.08 (s, 1H, CH_2═CH−), 6.75−6.96 (m, 3H, Ar−H), 7.26−7.74 (m, 4H, Ar−H), 9.19 (s, 1H, Ar−NH−); ^{13}C NMR: 32.26 (S−CH_2−), 39.96 (−CH_2−Ar), 55.80 (Ar−OCH_3), 61.64 (Ar−O−CH_2−oxadiazole), 105.93, 112.70, 116.09, 116.69, 121.08, 123.42, 129.42, 123.81, 136.40, 137.32, 147.92, 150.10, 164.40. ESI (+ve): 490 [M + H]+; 492 [M+2 + H]+; elemental analyses for $C_{21}H_{20}BrN_3O_4S$ (calcd): C, 51.44; H, 4.11; N, 8.57; S, 6.54. Found: C, 51.46; H, 4.11; N, 8.52; S, 6.52.

*2-((5-((4-Allyl-2-methoxyphenoxy)methyl)-1,3,4-oxadiazol-2-yl)thio)-1-morpholinoethanone (**13**).* Recryst. solvent: dichloromethane-cyclohexane; yield: 70%, mp 84−86 °C, FT-IR (cm^{-1}): 2970, 2928, 1627, 1589, 1514, 1464, 1385, 1279, 1220, 1167, 1069, 1025, 843, 802, ^{1}H NMR: 3.38 (d, J = 6.4 Hz, Ar−CH_2−), 3.72−3.90 (m, 11H, morpholine ring protons, Ar−O−CH_3), 4.36 (s, 2H, S−CH_2−), 5.03−5.27 (m, 4H, CH_2═CH−, O−CH_2−), 5.76−6.25 (m, 1H, CH_2═CH−),

https://doi.org/10.1021/acsomega.3c00933
ACS Omega 2023, 8, 18811−18822

6.69−7.04 (m, 3H, Ar−H). ESI (+ve): 406.83 [M + H]+; $C_{19}H_{23}N_3O_5S$ (calcd): C, 56.28; H, 5.72; N, 10.36; S, 7.91. Obsd: 56.20; H, 5.75; N, 10.33; S, 7.90.

2-((5-((4-Allyl-2-methoxyphenoxy)methyl)-1,3,4-oxadiazol-2-yl)thio)-1-(piperidin-1-yl)ethanone (14). Recryst. solvent: dichloromethane-cyclohexane; yield: 64%, mp 82−84 °C, FT-IR (cm^{-1}): 3280, 2984, 2930, 1670, 1602, 1509, 1486, 1376, 1251, 1210, 1141, 1030, 964, 914. ^1H NMR: 1.18−2.89 (m, 10H, piperidine ring), 3.32 (d, J = 6.4 Hz, Ar−CH_2−), 3.84 (brds, 5H, Ar−O−CH_3, S−CH_2−), 4.98−5.22 (m, 4H, CH_2=CH−, O−CH_2−), 5.70−6.19 (m, 1H, CH_2=CH−), 6.64−6.98 (m, 3H, Ar−H). ESI (+ve): 404.25 [M + H]+; elemental analyses for $C_{20}H_{25}N_3O_4S$ (calcd): C, 59.53; H, 6.25; N, 10.41; S, 7.95. Found: C, 59.41; H, 6.20; N, 10.35; S, 7.92.

General Procedure for the Synthesis of Compounds 15−17. Compound **4** (0.005 mol) was taken in a 100 mL clean round-bottom flask and then added 50 mL of ethanol. To the mixture, suitable secondary amine (0.006 mol) and formaldehyde (0.006 mol) were added and the reaction was refluxed for 6−8 h. When the reaction completed, the mixture was concentrated under vacuum and poured on to the cold ice water (50 mL) and products were isolated by extracting with ethyl acetate (25 mL × 2). Finally, crude products were crystallized by ethanol.

*5-((4-Allyl-2-methoxyphenoxy)methyl)-3-(pyrrolidin-1-ylmethyl)-1,3,4-oxadiazole-2(3H) Thione (**15**).* Recryst. solvent: ethanol; yield: 65.46%, mp 134−136 °C, FT-IR (cm^{-1}): 2933, 1507, 1417, 1259, 1216, 1140, 1028, 912, 847, 804. ^1H NMR: 1.50−2.22 (m, 4H, pyrrolidine ring −CH_2−CH_2−), 2.35−2.59 (m, 4H, pyrrolidine ring, CH_2−N−CH_2), 3.30−3.70 (m, 4H, Ar−CH_2−, N−CH_2−N−), 3.88 (s, 3H, Ar−O−CH_3), 5.07−5.18 (m, 4H, CH_2=CH−, O−CH_2−), 5.76−6.14 (m, 1H, CH_2=CH−), 6.77−7.01 (m, 3H, Ar−H); ^{13}C NMR: 24.42, 39.81, 44.97, 55.85, 61.96, 112.85, 116.03, 117.44, 120.71, 137.17, 144.95, 146.06, 150.31, 158.29, 160.80, 177.80. ESI (+ve): 362.25 [M + H]+; elemental analyses for $C_{18}H_{23}N_3O_3S$ (calcd): C, 59.81; H, 6.41; N, 11.63; S, 8.87. Found: C, 59.78; H, 6.38; N, 11.60; S, 8.90.

*5-((4-Allyl-2-methoxyphenoxy)methyl)-3-(piperidin-1-ylmethyl)-1,3,4-oxadiazole-2(3H)thione (**16**).* Recryst. solvent: ethanol; yield: 63.50%, mp 138−140 °C, FT-IR (cm^{-1}): 2936, 1516, 1439, 1413, 1316, 1215, 1174, 1142, 1051, 805. ^1H NMR: 0.95−1.28 (m, 6H, piperidine protons), 3.24−3.40 (m, 6H, piperidine protons, Ar−CH_2−), 3.79−3.89 (brs, 3H (Ar−O−C$\underline{H}_3$) + 2H (−N−C$\underline{H}_2$−)), 5.0−5.19 (m, 4H, CH_2=CH−, O−CH_2−), 5.73−6.22 (m, 1H, CH_2=CH−), 6.68−6.99 (m, 3H, Ar−H); ESI (+ve): 376.92 [M + H]+; elemental analyses for $C_{19}H_{25}N_3O_3S$ (calcd): C, 60.78; H, 6.71; N, 11.19; S, 8.54. Found: C, 60.65; H, 6.73; N, 11.16; S, 8.52.

*5-((4-Allyl-2-methoxyphenoxy)methyl)-3-(morpholinomethyl)-1,3,4-oxadiazole-2(3H)-thione (**17**).* Recryst. solvent: ethanol; yield: 68%, mp 144−146 °C, FT-IR (cm^{-1}): 2907, 1512, 1465, 1417, 1342, 1260, 1225, 1142, 1058, 1027, 923, 808. ^1H NMR: 3.35−3.43 (m, 2H, −Ar−CH_2−), 3.72−3.92 (m, 11H, Ar−O−CH_3, morpholine protons), 5.11−5.21 (m, 4H, CH_2=CH−, O−CH_2−), 5.77−6.27 (m, 1H, CH_2=CH−), 6.71−7.03 (m, 3H, Ar−H), ^{13}C NMR: 39.87, 47.35, 48.09, 55.93, 61.84, 62.04, 112.87, 114.79, 116.07, 116.74, 120.79, 123.63, 137.19, 139.08, 147.43, 160.00, 166.22, 178.78. ESI (+ve): 378.05 [M + H]+; elemental analyses for $C_{18}H_{23}N_3O_4S$ (calcd): C, 57.28; H, 6.14; N, 11.13; S, 8.49. Found: 57.33; H, 6.16; N, 11.10; S, 8.48.

Antiproliferative Activity. The cytotoxicity study was performed on MCF-7, SKOV3, and PC-3 cancerous cells according to our published work by the MTT method. Doxorubicin was used as a positive control for comparison.[30]

In Vitro Thymidylate Synthase Enzymatic Assay. It was performed as per previously published work.[30] Pemetrexed was used as a reference drug.

Cell Cycle Analysis. It was performed as per previously published work.[30] The experimental method has been provided in the Supporting Information.

Apoptosis Analysis. It was performed as per previously published work.[30] The experimental method has been provided in the Supporting Information.

Statistical Analysis. Results are presented as mean ± SD, performed in triplicate. One-way ANOVA was used to determine statistical significance ($*p < 0.05$).

DFT and Docking Studies. They were performed as previously published work.[16] The experimental protocol is available in the Supporting Information.

■ ASSOCIATED CONTENT

Supporting Information

The Supporting Information is available free of charge at https://pubs.acs.org/doi/10.1021/acsomega.3c00933.

NMR (^1H and ^{13}C) and mass spectra of final compounds and methods for biological, docking, and computational studies (PDF)

■ AUTHOR INFORMATION

Corresponding Authors

Ahmed A. Elhenawy − *Chemistry Department, Faculty of Science, Al-Azhar Unuversity, Cairo 11751, Egypt;* orcid.org/0000-0003-2893-0376; Email: elhenawy_sci@hotmail.com

Mohammad Mahboob Alam − *Department of Chemistry, Faculty of Science, Al-Baha University, Al-Baha 65799, Kingdom of Saudi Arabia*; Email: mmalamchem@gmail.com

Authors

Syed Nazreen − *Department of Chemistry, Faculty of Science, Al-Baha University, Al-Baha 65799, Kingdom of Saudi Arabia*

Serag Eldin I. Elbehairi − *Department of Biology, Faculty of Science, King Khalid University, Abha 9004, Saudi Arabia; Cell Culture Laboratory, Egyptian Organization for Biological Products and Vaccines, VACSERA Holding Company, Giza 2311, Egypt*

Azizah M. Malebari − *Department of Pharmaceutical Chemistry, Faculty of Pharmacy, King Abdulaziz University, Jeddah 21589, Kingdom of Saudi Arabia*

Nuha Alghamdi − *Department of Chemistry, Faculty of Science, Al-Baha University, Al-Baha 65799, Kingdom of Saudi Arabia*

Reem F. Alshehri − *Chemistry Department, Faculty of Science and Art, Taibah University, Madinah 16857, Kingdom of Saudi Arabia*

Ali A. Shati − *Department of Biology, Faculty of Science, King Khalid University, Abha 9004, Saudi Arabia*

Nada M. Ali − *Department of Chemistry, Faculty of Science, Al-Baha University, Al-Baha 65799, Kingdom of Saudi Arabia*

https://doi.org/10.1021/acsomega.3c00933
ACS Omega 2023, 8, 18811−18822

Mohammad Y. Alfaifi − *Department of Biology, Faculty of Science, King Khalid University, Abha 9004, Saudi Arabia*

Complete contact information is available at: https://pubs.acs.org/10.1021/acsomega.3c00933

Notes

The authors declare no competing financial interest.

■ ACKNOWLEDGMENTS

The authors thank the Deanship of Scientific Research at King Khalid University for funding this work through large Groups (Project under grant number R.G.P.2/213/44). M.M.A., S.N., N.A., and N.M.A. are greatly thankful to Al-Baha University.

■ REFERENCES

(1) Huang, M.; Lu, J. J.; Ding, J. Natural Products in Cancer Therapy: Past, Present and Future. *Nat. Prod. Bioprospect.* **2021**, *11*, 5−13.

(2) Demain, A. L.; Vaishnav, P. Natural products for cancer chemotherapy. *Microb. Biotechnol.* **2011**, *4*, 687−699.

(3) Dzobo, K. The Role of Natural Products as Sources of Therapeutic Agents for Innovative Drug Discovery. *Compr. Pharmacol.* **2022**, *2*, 408−422.

(4) Lee, K. H. Discovery and development of natural product-derived chemotherapeutic agents based on a medicinal chemistry approach. *J. Nat. Prod.* **2010**, *73*, 500−516.

(5) Nicolaou, K. C.; Pfefferkorn, J. A.; Roecker, A. J.; Cao, G. Q.; Barluenga, S.; Mitchell, H. J. Natural Product-like Combinatorial Libraries Based on Privileged Structures. 1. General Principles and Solid-Phase Synthesis of Benzopyrans. *J. Am. Chem. Soc.* **2000**, *122*, 9939−9953.

(6) Alam, M. M. Synthesis and anticancer activity of novel Eugenol derivatives against breast cancer cells. *Nat. Prod. Res.* **2023**, *37*, 1632−1640.

(7) Al-Sharif, I.; Remmal, A.; Aboussekhra, A. Eugenol triggers apoptosis in breast cancer cells through E2F1/survivin down-regulation. *BMC Cancer* **2013**, *13*, 600−610.

(8) Rohane, S. H.; Chauhan, A. J.; Fuloria, N. K.; Fuloria, S. Synthesis and in vitro antimycobacterial potential of novel hydrazones of Eugenol. *Arabian J. Chem.* **2020**, *13*, 4495−4504.

(9) Kamatou, G. P.; Vermaak, I.; Viljoen, A. M. Eugenol—From the Remote Maluku Islands to the International Market Place: A Review of a Remarkable and Versatile Molecule. *Molecules* **2012**, *17*, 6953−6981.

(10) Choudhury, P.; Barua, A.; Roy, A.; Pattanayak, R.; Bhattacharyya, M.; Saha, P. Eugenol restricts Cancer Stem Cell population by degradation of β-catenin via N-terminal Ser37 phosphorylation-an in vivo and in vitro experimental evaluation. *Chem.-Biol. Interact.* **2020**, *316*, 108938.

(11) Yoo, C. B.; Han, K. T.; Cho, K. S.; Ha, J.; Park, H. J.; Nam, J. H.; Kil, U. H.; Lee, K. T. Eugenol isolated from the essential oil of Eugenia caryophyllata induces a reactive oxygen species-mediated apoptosis in HL-60 human promyelocytic leukemia cells. *Cancer Lett.* **2005**, *225*, 41−52.

(12) Shin, S. H.; Park, J. H.; Kim, G. C. The mechanism of apoptosis induced by Eugenol in human osteosarcoma cells. *J. Korean Assoc. Oral Maxillofac. Surg.* **2007**, *33*, 20−27.

(13) Abdullah, M. L.; Hafez, M. M.; Al-Hoshani, A.; Al-Shabanah, O. Anti-metastatic and anti-proliferative activity of Eugenol against triple negative and HER2 positive breast cancer cells. *BMC Complementary Altern. Med.* **2018**, *18*, 321−332.

(14) Siegel, R. L.; Miller, K. D.; Wagle, N. S.; Jemal, A. Cancer statistics, 2023. *Ca-Cancer J. Clin.* **2023**, *73*, 17−48.

(15) Chon, J.; Stover, P. J.; Field, M. S. Targeting nuclear thymidylate biosynthesis. *Mol. Aspects Med.* **2017**, *53*, 48−56.

(16) Alam, M. M.; Malebari, A. M.; Nazreen, S.; Neamatallah, T.; Almalki, A. S. A.; Elhenawy, A. A.; Obaid, R. J.; Alsherif, M. A. Design, synthesis and molecular docking studies of thymol based 1,2,3-triazole hybrids as thymidylate synthase inhibitors and apoptosis inducers against breast cancer cells. *Bioorg. Med. Chem.* **2021**, *38*, 116136.

(17) Hanauske, A. R.; Eismann, U.; Oberschmidt, O.; Pospisil, H.; Hoffmann, S.; Hanauske-Abel, H.; Ma, D.; Chen, V.; Paoletti, P.; Niyikiza, C. In vitro chemosensitivity of freshly explanted tumor cells to Pemetrexed is correlated with target gene expression. *Invest. New Drugs* **2007**, *25*, 417−423.

(18) Roukos, D. H.; Katsios, C.; Liakakos, T. Genotype-phenotype map and molecular networks: a promising solution in overcoming colorectal cancer resistance to targeted treatment. *Expert Rev. Mol. Diagn.* **2010**, *10*, 541−545.

(19) Wang, Y.; Mitchell-Ryan, S.; Raghavan, S.; George, C.; Orr, S.; Hou, Z.; Matherly, L. H.; Gangjee, A. Novel 5-Substituted Pyrrolo[2,3-d]pyrimidines as Dual Inhibitors of Glycinamide Ribonucleotide Formyltransferase and 5-Aminoimidazole-4-carboxamide Ribonucleotide Formyltransferase and as Potential Antitumor Agents. *J. Med. Chem.* **2015**, *58*, 1479−1493.

(20) Wilson, P. M.; Fazzone, W.; LaBonte, M. J.; Deng, J.; Neamati, N.; Ladner, R. D. Novel opportunities for thymidylate metabolism as a therapeutic target. *Mol. Cancer Ther.* **2008**, *7*, 3029−3037.

(21) Benassi, A.; Doria, F.; Pirota, V. Groundbreaking Anticancer Activity of Highly Diversified Oxadiazole Scaffolds. *Int. J. Mol. Sci.* **2020**, *21*, 8692−8720.

(22) Zheng, Q.-Z.; Zhang, X.-M.; Xu, Y.; Cheng, K.; Jiao, Q.-C.; Zhu, H.-L. Synthesis, biological evaluation, and molecular docking studies of 2-chloropyridine derivatives possessing 1,3,4-oxadiazole moiety as potential antitumor agents. *Bioorg. Med. Chem.* **2010**, *18*, 7836−7841.

(23) Rajak, H.; Agarawal, A.; Parmar, P.; Thakur, B. S.; Veerasamy, R.; Sharma, P. C.; Kharya, M. D. 2,5-Disubstituted-1,3,4-oxadiazoles/thiadiazole as surface recognition moiety: Design and synthesis of novel hydroxamic acid based histone deacetylase inhibitors. *Bioorg. Med. Chem. Lett.* **2011**, *21*, 5735−5738.

(24) Zhang, S.; Luo, Y.; He, L.-Q.; Liu, Z.-J.; Jiang, A.-Q.; Yang, Y.-H.; Zhu, H.-L. Synthesis, biological evaluation, and molecular docking studies of novel 1,3,4-oxadiazole derivatives possessing benzotriazole moiety as FAK inhibitors with anticancer activity. *Bioorg. Med. Chem.* **2013**, *21*, 3723−3729.

(25) Du, Q. R.; Li, D. D.; Pi, Y. Z.; Li, J. R.; Sun, J.; Fang, F.; Zhong, W. Q.; Gong, H. B.; Zhu, H. L. Novel 1,3,4-oxadiazole thioether derivatives targeting thymidylate synthase as dual anticancer/antimicrobial agents. *Bioorg. Chem.* **2013**, *21*, 2286−2297.

(26) Popov, S.; Semenova, M. D.; Baev, D. S.; Frolova, T. S.; Shestopalov, M. A.; Wang, C.; Qi, Z.; Shults, E. E.; Turks, M. Synthesis and cytotoxicity of hybrids of 1,3,4- or 1,2,5-oxadiazoles tethered from ursane and lupane core with 1,2,3-triazole. *Steroids* **2020**, *162*, 108698.

(27) Ren, J.; Wu, L.; Xin, W. Q.; Chen, X.; Hu, K. Synthesis and biological evaluation of novel 4β-(1,3,4-oxadiazole-2-amino)-podophyllotoxin derivatives. *Bioorg. Med. Chem. Lett.* **2012**, *22*, 4778−4782.

(28) Alam, M. M.; Elbehairi, S. E. I.; Shati, A. A.; Hussien, R. A.; Alfaifi, M. Y.; Malebari, A. M.; Asad, M.; Elhenawy, A. A.; Asiri, A. M.; Mahzari, A. M.; Alshehri, R. F.; Nazreen, S. Design, synthesis and biological evaluation of new eugenol derivatives containing 1,3,4-oxadiazole as novel inhibitors of thymidylate synthase. *New J. Chem.* **2023**, *47*, 5021−5032.

(29) Almalki, A. S. A.; Nazreen, S.; Malebari, A. M.; Ali, N.; Elhenawy, A. A.; Alghamdi, A. A.; Ahmad, A.; Alfaifi, S. Y. M.; Alsharif, M. A.; Alam, M. M. Synthesis and Biological Evaluation of 1,2,3-Triazole Tethered Thymol-1,3,4-Oxadiazole Derivatives as Anticancer and Antimicrobial Agents. *Pharmaceuticals* **2021**, *14*, 866−886.

(30) Mironov, M. E.; Pokrovsky, M. A.; Kharitonov, Y. V.; Shakirov, M. M.; Pokrovsky, A. G.; Shults, E. E. Furanolabdanoid−based 1,2,4-oxadiazoles: Synthesis and cytotoxic activity. *ChemistrySelect* **2016**, *1*, 417−424.

(31) Liu, C.-J.; Zhang, T.; Yu, S.-L.; Dai, X.-J.; Wu, Y.; Tao, J.-C. Synthesis, cytotoxic activity, and 2D- and 3D-QSAR studies of 19-carboxyl-modified novel isosteviol derivatives as potential anticancer agents. *Chem. Biol. Drug Des.* **2017**, *89*, 870−887.
(32) Alzahrani, H. A.; Alam, M. M.; Elhenawy, A. A.; Malebari, A. M.; Nazreen, S. Synthesis, antiproliferative, docking and DFT studies of benzimidazole derivatives as EGFR inhibitors. *J. Mol. Struct.* **2022**, *1253*, 132265−132313.
(33) Nazreen, S.; Almalki, A. S. A.; Elbehairi, S. E. I.; Shati, A. A.; Alfaifi, M. Y.; Elhenawy, A. A.; Alsenani, N. I.; Alfarsi, A.; Alhadhrami, A.; Alqurashi, E. A.; Alam, M. M. Cell Cycle Arrest and Apoptosis-Inducing Ability of Benzimidazole Derivatives: Design, Synthesis, Docking, and Biological Evaluation. *Molecules* **2022**, *27*, 6899−6912.
(34) Ligabue, A.; Marverti, G.; Liebl, U.; Myllykallio, H. Transcriptional Activation and Cell Cycle Block Are the Keys for 5-Fluorouracil Induced Up-Regulation of Human Thymidylate Synthase Expression. *PLoS One* **2012**, *7*, No. e47318.
(35) Li, X. Y.; Zhang, T. J.; Kamara, M. O.; Lu, G. Q.; Xu, H. L.; Wang, D. P.; Meng, F. H. Discovery of N-phenyl-(2,4-dihydroxypyrimidine-5-sulfonamido) phenylurea-based thymidylate synthase (TS) inhibitor as a novel multi-effects antitumor drugs with minimal toxicity. *Cell Death Dis.* **2019**, *10*, 532−547.
(36) http://www.swissadme.ch/ (accessed on Jan 18, 2023) .

https://doi.org/10.1021/acsomega.3c00933
ACS Omega 2023, 8, 18811−18822